The neutron diffraction study, calorimetry and spontaneous polarization of pyridinium perrhenate at 350, 300 and 100 K

2010 J. Phys.: Condens. Matter 22 235901

(http://iopscience.iop.org/0953-8984/22/23/235901)

J. Phys.: Condens. Matter **22** (2010) 235901 (8pp) doi:10.1088/0953-8984/22/23/235901

The neutron diffraction study, calorimetry and spontaneous polarization of pyridinium perrhenate at 350, 300 and 100 K

Hanna Małuszyńska[1,3], Alain Cousson[2] and Piotr Czarnecki[1]

[1] Physics Department, Adam Mickiewicz University, Umultowska 85, 61-614 Poznań, Poland
[2] Laboratoire Léon Brillouin (CEA-CNRS), CEA Saclay, F-91191 Gif-sur-Yvette Cedex, France

E-mail: hanmal@amu.edu.pl

Received 2 February 2010, in final form 30 April 2010
Published 21 May 2010
Online at stacks.iop.org/JPhysCM/22/235901

Abstract

The crystal and molecular structure of pyridinium perrhenate $[H_5C_5NH]^+$ $[ReO_4]^-$ (hereafter referred to as $PyReO_4$) was determined by single-crystal neutron diffraction at 350, 300 and 100 K. The neutron study confirmed the x-ray diffraction results in all three phases. The three temperature-dependent polymorphs are orthorhombic, with the following sequence of phases: $Cmcm \longrightarrow Cmc2_1 \longrightarrow Pbca$, with the a lattice parameter doubled. In the two high temperature phases the pyridinium cations display a rotational disorder while the perrhenate anions are well ordered. The low temperature phase is fully ordered. The neutron results allow for a very precise description of the distribution of the nitrogen atoms in the disordered pyridinium cation, which enables us to analyse the calorimetric and spontaneous polarization measurements. The results from the DSC and pyroelectric measurements point to a paraelectric (350 K), ferroelectric (300 K) with the Curie point at 336 K and antiferroelectric (100 K) crystal phases. The phase transition at 336 K can be classified as an order–disorder ferroelectric with a small displacive component.

(Some figures in this article are in colour only in the electronic version)

1. Introduction

Pyridinium salts belong to a group of molecular–ionic complexes in which polymorphic solid–solid phase transitions have been revealed by extensive DSC, x-ray and neutron diffraction, NMR and dielectric spectroscopy studies [1–7]. These phase transitions are evidently related to the molecular dynamics of the pyridinium cation and of halide anions and BF_4, ClO_4, ReO_4, IO_4, FSO_3 and $FCrO_3$ tetrahedral anions. It was also found that the number of phase transitions in these molecular–ionic crystals depends entirely on the type and structure of the anions. The most interesting physical property, like ferroelectricity, was discovered in mesophases of pyridinium salts in which at least two or more phase transitions take place and whose anions display a tetrahedral symmetry. Properties of new ferroelectrics, especially if their Curie point is close to room temperature, are the subject of intensive studies due to their possible application in electronics and optics as well as basic scientific concerns [8–13].

The family of these pyridinium ferroelectrics crystals can be divided into two subgroups according to the symmetry of their prototype high temperature phase. The first subgroup is of pyridinium salts with trigonal symmetry (with ClO_4, BF_4 and FSO_3 ions), while the second subgroup comprises salts with orthorhombic symmetry of their prototype phase (with ReO_4, IO_4 and $FCrO_3$ ions).

Pyridinium perrhenate $[H_5C_5NH]^+ReO_4^-$, hereafter referred to as $PyReO_4$, belongs to pyridinium salts with the recently discovered ferroelectric properties in at least one of their three temperature-dependent polymorphs [3, 4]. $PyReO_4$, together with pyridinium periodate ($PyIO_4$) and

[3] Author to whom any correspondence should be addressed.

Table 1. Crystal data and structure refinement for $[H_5C_5NH]^+ReO_4^-$ at 350, 300 and 100 K.

Temperature	350 K	300 K	100 K
Formula weight	330.3	330.3	330.3
Crystal system	*Cmcm*	$Cmc2_1$	*Pbca*
Unit cell (Å)	$a = 8.415(1)$	8.40(2)	17.012(3)
	$b = 7.379(1)$	7.27(2)	7.259(1)
	$c = 12.511(1)$	12.45(4)	12.118(2)
Volume (Å^3)	776.9(1)	760(4)	1496.5(4)
Wavelength (Å)	0.8292	0.8370	0.8292
Z, density (Mg m^{-3})	4, 2.823	4, 2.885	8, 2.931
Absorption (mm^{-1})	0.275	0.275	0.275
Crystal size (mm)	$4 \times 5 \times 6$	$3 \times 4 \times 5$	$4 \times 5 \times 6$
Theta range	3.80–42.53	3.85–45.31	2.79–42.68
Reflections collected, unique, R (int.)	734, 733, 0.0	1723, 983, 0.07	3160, 2795, 0.13
Refinement method	Full matrix least-squares on F^2		
Data/restraints/parameters	733/4/50	983/0/89	2795/0/155
Goodness of fit on F^2	1.029	0.852	1.454
Final R indices $I > 3\sigma(I)$	$R_1 = 0.0542$	$R_1 = 0.0456$	$R_1 = 0.0803$
	$wR_2 = 0.1368$	$wR_2 = 0.1095$	$wR_2 = 0.2130$
Largest diff. peak and hole (e Å^{-3})	0.33 and −0.33	0.66 and −0.58	1.78 and −1.82

The CCDC reference numbers of the CIF files of the three phases are 776864-776866.

pyridinium fluorochromate ($PyFCrO_3$), belongs to a second subgroup of pyridinium ferroelectric salts which crystallize in an orthorhombic system in the *Cmcm* space group of their prototype high temperature phase [4–7]. The intermediate ferroelectric phase of all three compounds is orthorhombic, with $Cmc2_1$ space group. Both high and room temperature phases of $PyReO_4$ [4], $PyIO_4$ [5, 6] and $PyFCrO_3$ [7] are isostructural with disordered pyridinium cations and ordered, except for $PyFCrO_3$, anions. The low temperature phase of these compounds is well ordered but only $PyReO_4$ [4] and $PyFCrO_3$ [7] are known to be orthorhombic and centrosymmetric (with *Pbca* space group and with the lattice parameter a doubled). The very precise single-crystal neutron diffraction data on $PyIO_4$ [6] have shown that below the second phase transition the $PyIO_4$ changes the system to monoclinic and the space group to $C112_1$, preserving the ferroelectric properties.

The structure of $PyReO_4$ has been studied only by the x-ray diffraction method at 350 K, RT and 220 K [4] and the obtained structural results were strongly biased by large absorption. This concerns not only the symmetry and the space group of the LT phase but also the precise bond lengths and angles in all three phases. We decided to undertake the neutron diffraction study of $PyReO_4$ not only to determine the correctness of the space group of the LT phase, but also to find the distribution of the nitrogen atoms in the pyridinium cation in all three phases. The accurate values of the occupancy factor of the N atom of the cation are crucial for the model of the disorder of the pyridinium cation and for an explanation of the origin of the ferroelectricity in this compound. They are also essential for understanding the mechanism of phase transition in the $PyReO_4$.

In this paper we present the results of accurate structural investigation by neutron diffraction at 350, 300 and 100 K of a single crystal of $PyReO_4$ and a mechanism for the phase transitions. We also present the DSC study with entropy changes and pyroelectric measurements together with theoretical calculations of spontaneous polarization which allowed us to establish a more precise model of ferroelectricity in this compound.

2. Experimental details

The pyridinium perrhenate was prepared by allowing the pyridinium base dissolved in 50% ethanol to react with perrhenic acid obtained by dissolving rhenium oxide in water. The product recrystallized from 50% ethanol was dried and ground to powder. The crystals were grown from water solution by slow evaporation at constant temperature.

Neutron diffraction studies were carried out on the 5C2 four-circle diffractometer located on the hot source of the ORPHEE reactor at the LLB in Saclay, France. The wavelength used was selected by the horizontally focusing Cu(220) monochromator and the harmonic $\lambda/2$ contamination was attenuated to 10^{-3} by an erbium filter. The intensities of reflections were measured using the ω-scan. An Oxford Instruments liquid helium evaporation cryostat was used at 100 K and a special furnace adapted for the diffractometer at 350 K. The temperatures were maintained within ±1 K. The crystal with dimensions of 4 mm × 5 mm × 6 mm, in aluminium foil, was glued with its c axis parallel to the φ axis of the Eulerian cradle and with the ψ angle equal to zero for all temperatures. No significant changes of intensities were observed for two standard reflections.

Data reduction was carried out using the PRON2K[3] program and the structures were solved and refined using SHELXS [14] and SHELXL-97 [15], respectively. A summary of crystallographic and computational details is given in table 1.

Heat capacity measurements were carried out by differential scanning calorimetry (DSC) on a Q2000 (TA Instruments) calorimeter. The DSC runs were recorded upon

[3] PRON2K, DATA REDUCTION FOR STOE 'DIF4', version for the Institut für Kristallographie, RWTH Aachen.

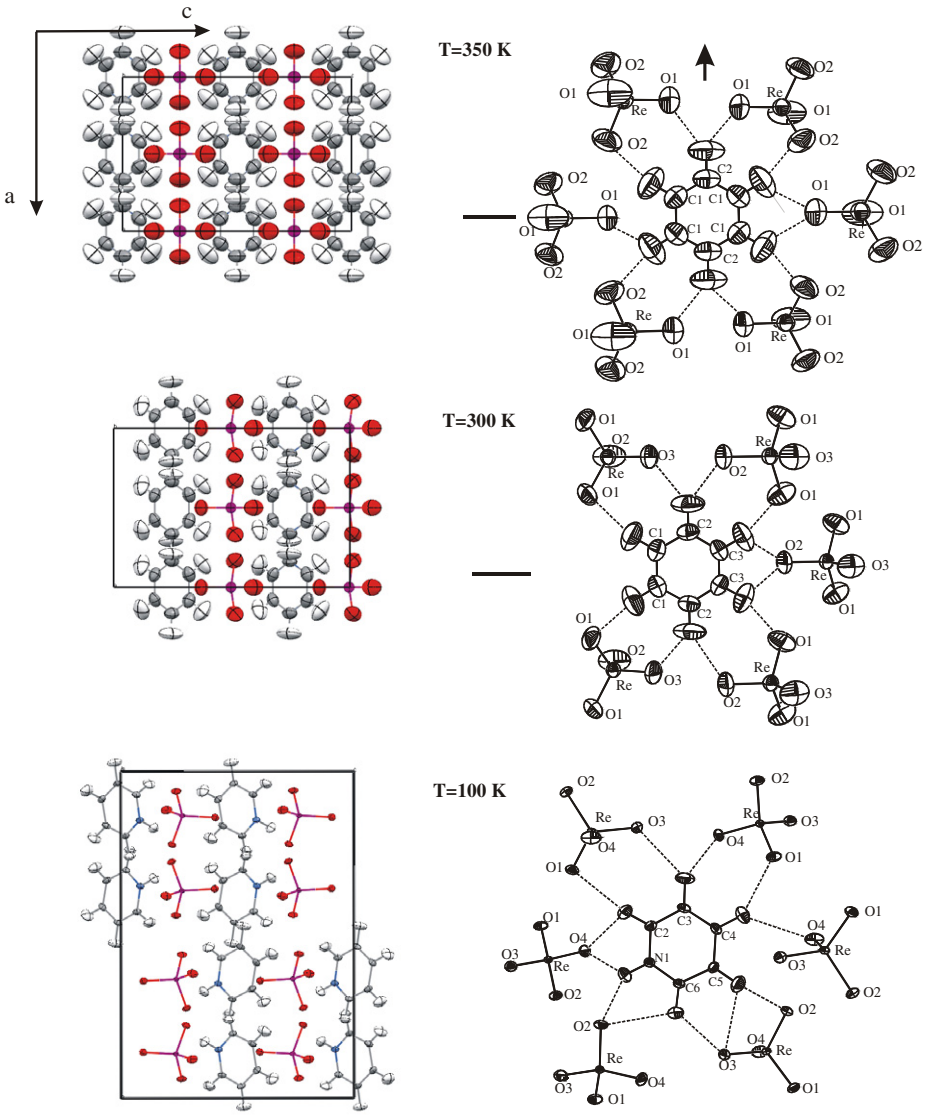

Figure 1. Crystal structure of $PyReO_4$ (left) in three phases down the *b* axis. On the right there are ORTEP drawings at 50% probability of the perrhenate anions around the pyridinium cation.

heating and cooling polycrystalline samples of 7.8 mg weight at a rate of 10 K min^{-1}. An indium standard was used for temperature and enthalpy calibration, and synthetic sapphire was used for heat capacity calibration.

The spontaneous polarization was obtained from measurements of the pyroelectric effect made using a Keithley-type 6514 electrometer. For the pyroelectric measurements x-ray-oriented samples of 0.5 mm in thickness and 4 mm^2 in area were used. The measurements were performed along the polar direction (0 0 1) between 190 and 350 K.

3. Results and discussion

3.1. Neutron diffraction

The neutron results confirmed the structure of the three phases of $PyReO_4$ determined by the x-ray diffraction method [4] and the sequence of phases: $Cmcm(350\ K) \longrightarrow Cmc2_1(RT) \longrightarrow Pbca$ (100 K). The crystal structure of $PyReO_4$ in three phases together with ORTEP drawings are presented in figure 1.

As determined by the x-ray measurements in the HT phase the pyridinium cation located at the $2/m$ site is disordered while the perrhenate ion located at the *mm* site is ordered. The neutron refinement converged at 5.42% and allowed us not only to find the hydrogen atoms' location and their full anisotropic refinement but, what is more important, to obtain a distribution of the nitrogen atom over six carbon atoms in the pyridinium ring. (In the x-ray results it was assumed, that all six atoms in the pyridinium ring are carbons.) At 350 K the refinement of the occupancy factors of the nitrogen and carbon atoms with appropriate constraints imposed by the $2/m$ symmetry results in very interesting values: 16.7(7)% of the N atom at C(1) and C(2). That means that, regardless of the $2/m$ symmetry site at which the pyridinium ring is

Table 2. The hydrogen bonds in $PyRO_4$ at 350 K, 300 K and 100 K.

Donor	Acceptor	H···O (Å)	D···A (Å)	∠D–HO (deg)	Symmetry operation
			$T = 350$ K		
C(1)–H(1)	O(2)	2.307(8)	3.334(6)	160.1(6)	$x + 1/2, y - 1/2, z$
C(2)–H(2)	O(1)	2.484(9)	3.329(6)	135.9(2)	$-x + 1/2, -y + 3/2, -z + 1$
			$T = 300$ K		
C(1)–H(1)	O(1)	2.39(1)	3.437(10)	161.0(1.4)	$-x - 1/2, y + 1/2, z$
C(2)–H(2)	O(3)	2.40(2)	3.256(10)	135.4(2.2)	$x - 1/2, y + 1/2, z$
C(2)–H(2)	O(2)	2.57(3)	3.416(10)	135.0(2.1)	$-x - 1/2, -y + 1/2, z - 1/2$
C(3)–H(3)	O(1)	2.197(17)	3.193(11)	157.5(1.6)	$-x - 1/2, -y + 1/2, z - 1/2$
C(3)–H(3)	O(2)	2.463(23)	3.010(13)	111.4(1.4)	$-x, -y, z - 1/2$
			$T = 100$ K		
N(1)–H(1)	O(2)	2.022(9)	2.897(4)	141.4(7)	$x + 1/2, -y + 1, z + 1/2$
N(1)–H(1)	O(4)	2.139(9)	2.829(4)	122.7(7)	$x, -y + 1/2, z + 1/2$
C(2)–H(2)	O(4)	2.388(9)	2.969(5)	111.5(6)	$x, -y + 1/2, z + 1/2$
C(2)–H(2)	O(1)	2.477(9)	3.053(5)	158.5(7)	$-x, -y + 1, -z$
C(3)–H(3)	O(3)	2.542(10)	3.386(5)	133.5(8)	$-x, -y + 1, -z$
C(4)–H(4)	O(1)	2.384(10)	3.337(5)	144.8(8)	$-x, y - 1/2, -z - 1/2$
C(5)–H(5)	O(2)	2.377(10)	3.334(5)	146.8(9)	$-x + 1/2, y - 1/2, z$
C(6)–H(6)	O(3)	2.427(9)	3.150(5)	123.7(7)	$-x + 1/2, y - 1/2, z$
C(6)–H(6)	O(2)	2.788(10)	3.253(5)	106.1(6)	$-x + 1/2, -y + 1, z + 1/2$

located, the distribution of the nitrogen atom is 1/6 over each of the six carbon atoms. This result is very different from the neutron data of the pyridinium periodate where, in the HT phase, isostructural with the HT phase of this compound, the occupancy factor of the nitrogen atom at C(1) and C(2) was 6.3(2)% and 21.9(1)%, respectively [6]. Our results are consistent with the ^{1}H NMR study of $PyReO_4$ [3], where the disorder of the pyridinium cation at 350 K is explained as in-plane 60° jumps around a pseudo-hexagonal axis perpendicular to the ring plane. The mean Re–O, C–C and C–H bond lengths are 1.697(6), 1.365(7) and 1.078(8) Å, respectively, and the last two values agree well with their equivalents reported in the $PyIO_4$ salt.

At 333 K the $PyReO_4$ undergoes a weak second-order/continuous ferroelectric phase transition into the non-centrosymmetric space group $Cmc2_1$. The neutron data at 300 K confirmed the previous structural results. The disordered pyridinium cation and ordered perrhenate anion are located at the *m* site. In this ferroelectric intermediate phase the N distribution is more localized: there is a 4.5(5)% occupation probability for the N atom at C(1), 3.0(7)% at C(2) and 42.5(7)% at C(3) sites. It is interesting to notice that the C(3) site, where the largest part of the N atom is located in this ferroelectric phase, becomes an N atom in the fully ordered LT phase at 100 K. The corresponding values obtained from the neutron diffraction analysis of $PyIO_4$ in this intermediate ferroelectric phase are 8.6(3), 6.9(3) and 34.5(3)%, respectively [6], and suggest that in $PyReO_4$ the N atom is more localized. The Re–O bond lengths range from 1.690(11) to 1.707(6) Å and they are equal within experimental error, but the non-equal distribution of the N atom in the pyridinium ring gives rise to one shorter C(3)/N–C(3)/N bond of 1.326(11) Å and three longer bonds, from 1.363–1.381 Å. The shortest C(3)–H(3) bond of 1.050 Å (versus 1.085 and 1.072 Å) is also consistent with the 42.5(7)% occupation probability for the N atom at the C(3) site.

At 255 K the $PyReO_4$ undergoes a relatively strong first-order/discontinues phase transition, the C-centring vanishes and the space group becomes *Pbca* with the *a* lattice parameter doubled.

The neutron diffraction data studied at 100 K fully confirmed the x-ray results which, as mentioned in section 1, were strongly biased by large absorption [4]. The *Pbca* space group is centrosymmetric and the $PyReO_4$ in the LT phase loses its ferroelectric properties, becoming an antiferroelectric. Both ions are fully ordered with localized nitrogen atom, which forms a bifurcated hydrogen bond to O2 and O4 (from two different perrhenate ions) with the geometry given in table 2.

Although two high temperature phases of $PyReO_4$ and $PyIO_4$ are isostructural, the LT phases of these two pyridinium salts are quite different. The perrhenate salt remains orthorhombic, with *Pbca* space group, while the periodate compound changes into a monoclinic system with $C112_1$ space group. Surprisingly this LT antiferroelectric phase of $PyReO_4$ is isostructural with $PyFCrO_3$ in which the $FCrO_3$ anion is much smaller and more asymmetric than ReO_4. Additionally the H bond pattern and the non-bonded interactions, which occur in this LT phase (see table 2), are very similar to those observed in the corresponding LT phase of the $PyFCrO_3$ [7].

In the LT phase of $PyReO_4$ both ions are located in a general position, so there are no symmetry related atoms within the ions. The Re–O bond lengths range from 1.730 to 1.740(4) Å with a mean of 1.735(4) Å and O–Re–O angles from 109.2 to 109.9(2)° show that the perrhenate ion is almost an ideal tetrahedron, which is not the case in the periodate ion of the LT phase of the $PyIO_4$, where one of the I–O bonds involved in the N–H···O hydrogen bond is significantly longer (1.791(6) Å versus 1.770(4), 1.772(4) and 1.756(6) Å) and some of the O–I–O angles differ significantly

Table 3. A summary of the phase transitions in three pyridinium salts.

Compound	HT paraelectric	T_1 Curie point (K)	RT ferroelectric	T_2 (K)	LT	Geometry of the anion
$PyIO_4$ [6]	*Cmcm* (350 K)	321	$Cmc2_1$ (300 K)	210	$C112_1$ (100 K) ferroelectric	1.756–1.781 Å very asymmetric
$PyReO_4$ this work	*Cmcm* (350 K)	336	$Cmc2_1$ (300 K)	255	*Pbca* (100 K) antiferroelectric	1.730–1.740 Å almost symmetric
$PyFCrO_3$ [7]	*Cmcm* (300 K)	258	$Cmc2_1$ (240 K)	224	*Pbca* (150 K) antiferroelectric	1.628–1.695 Å very asymmetric

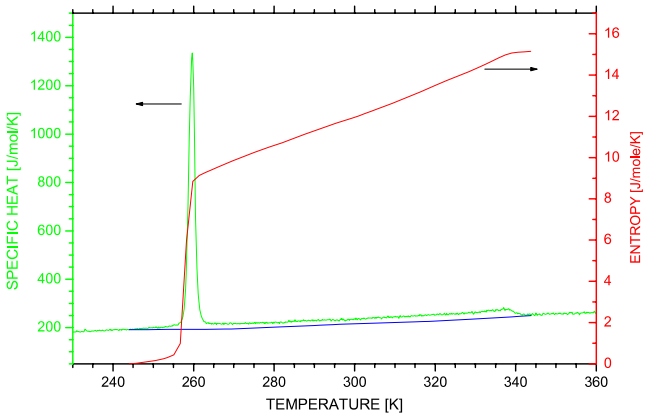

Figure 2. The specific heat (left scale) and the entropy change (right scale) versus temperature.

from 109.5° [6]. All bond lengths and angles in the pyridinium cation are in the range of their expected values (the mean N_{sp2}–C_{sp2} of 1.340(4) Å, mean C_{sp2}–C_{sp2} of 1.392(5) Å and mean C–H of 1.086(9) Å) and agree well with the corresponding values reported in the $PyIO_4$ [6].

A summary of the phase transition in these three pyridinium salts, mainly $PyIO_4$, $PyReO_4$ and $PyFCrO_3$, are given in table 3.

Two high temperature phases of these three pyridinium salts are isostructural with different Curie points and with small differences in the distribution of the nitrogen atom of the pyridinium ring. But why these three isostructural compounds in two high temperature phases behave so differently in the LT phases remains unclear. One of the possible explanations may be a different size, geometry and a different electronic structure of the periodate, perrhenate and fluorochromate ions (the periodate ion is the biggest), differences in the non-bonded interactions and a stronger and more directional hydrogen bond in the $PyIO_4$ than in the $PyReO_4$ and $PyFCrO_3$ observed in the LT phases.

3.2. Entropy analysis

The result of DSC specific heat C_p measurements and entropy changes as a function of temperature is presented in figure 2. The anomalies in the temperature dependence of the specific heat indicate the occurrence of two phase transitions in $PyReO_4$, one at $T_1 = 336$ K and the other one at $T_2 = 258$ K.

The large anomaly of specific heat at $T_2 = 258$ K is associated with a discontinuous phase transition while a small anomaly at $T_1 = 336$ K is characteristic for a continuous one.

The transition entropy was calculated using

$$\Delta S = \int_{T_{\min}}^{T} \frac{C_p - C_b}{T}\,\mathrm{d}T, \tag{1}$$

where C_p is a heat capacity obtained by the DSC method, C_b is a baseline (figure 2), and T and $T_{\min}$ is the temperature range.

The entropy change connected with a phase transition is an important parameter in a description of the origin of a phase transition. Usually when the entropy change is larger than 2 J mol^{-1} K^{-1} the phase transition is considered as an order–disorder type.

The total entropy change ΔS of the two phase transitions was estimated using (1) as about 15 J mol^{-1} K^{-1}. This total entropy change ΔS can be divided into two components: one originated from the continuous phase transition at $T_1 = 336$ K between HT and RT (ΔS_1) and a second component originated from the RT and LT phases (ΔS_2):

$$\Delta S = \Delta S_1 + \Delta S_2. \tag{2}$$

The entropy change in the order–disorder phase transitions can be evaluated from the formula

$$\Delta S = R \ln(N_I/N_{II}), \tag{3}$$

where ΔS is the entropy change, N_I and N_{II} are the numbers of the independent positions with equal probability in the crystal phases above and below the phase transition temperature and R is the gas constant.

If the positions of the atoms/molecules in the disordered phase occur with non-equal probability, e.g. the molecules and atoms have non-equal occupancy factor, the entropy change is given in [16]:

$$\Delta S = R\Sigma p_i \ln(1/p_i) - R\Sigma P_j \ln(1/P_j), \tag{4}$$

where p_i and P_j are the probability of the population of the i position in the disordered phase and of the j position in the ordered phase, respectively.

In $PyReO_4$ there is an orientational disorder of the pyridinium cation. The neutron diffraction results allow for a very precise description of the nitrogen atom distribution within the pyridinium cation, which means they allow us to obtain the probability p_i and P_j in the three phases. The distribution of the p_i and P_j of the nitrogen atom in three phases obtained from the neutron data are presented in figure 3.

In the HT phase the probability $p_i = 0.16$ is equal in the six positions of the aromatic ring, which suggests that

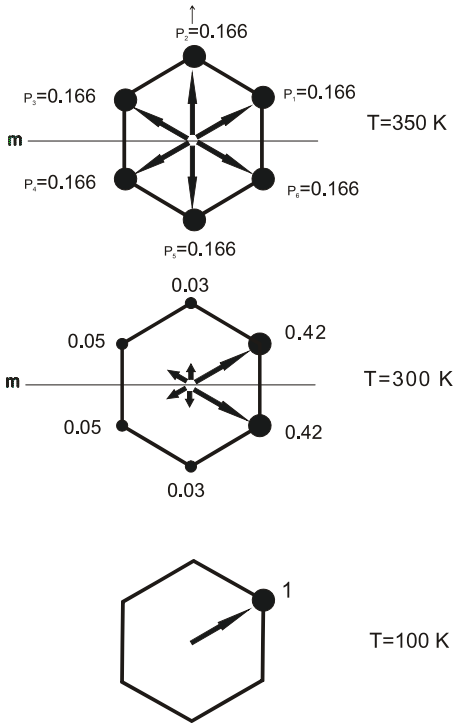

Figure 3. The distribution of the nitrogen atom in the pyridinium cation in three crystal phases. The numbers are the probability of the population of the nitrogen atom with a pyridinium ring. The arrows denotes the orientations of the dipole moments.

the pyridinium cation can occupy any of the six positions with equal probability. From the NMR studies [3] the in-plane reorientations of the cation are postulated. Therefore we can conclude that the pyridinium cation undergoes reorientational jumps about 60° around the pseudo-hexagonal axis perpendicular to the pyridinium plane through the equivalent barriers of the potential energy.

In the RT phase two of the six positions of the pyridinium ring have the highest population of the nitrogen atom (figure 3) and in this phase the reorientations take place mainly between these two positions. In the LT phase the cation is well ordered and the pyridinium ring occupies only one position in the asymmetric unit.

Having the probabilities p_i of the nitrogen atom in the HT and RT phases the entropy change between these phases using (4) was calculated. The obtained value of $S_1 = 4.5$ J mol^{-1} K^{-1} remains in good agreement with the entropy change calculated according to (1) with the experimental C_p (figure 2) value. The entropy change between the RT and LT phases calculated as above is equal to $\Delta S_2 = 10.3$ J mol^{-1} K^{-1} and also agrees with the value obtained experimentally from C_p (figure 2). The relatively high value of ΔS_2 confirms that the RT phase should be considered as disordered. So the transition from disordered HT phase to fully ordered LT phase takes place through the partly ordered ferroelectric RT phase.

The total entropy change $\Delta S = \Delta S_1 + \Delta S_2$ of the two phase transitions calculated using (4) is equal to 14.8 J mol^{-1} K^{-1} and is in good agreement with the experimentally obtained value of 15.1 J mol^{-1} K^{-1} from the C_p measurements (figure 2).

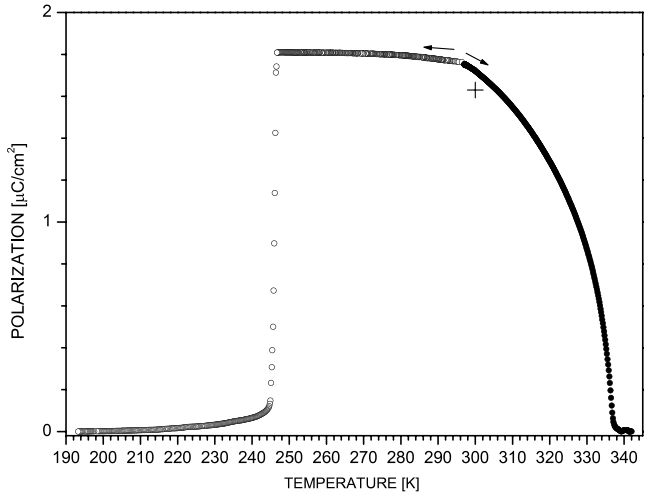

Figure 4. Spontaneous polarization obtained on the basis of pyroelectric charge measurements during cooling (open symbols) and heating (full symbols). The theoretical calculated value of spontaneous polarization is marked by a cross.

3.3. Spontaneous polarization of the ferroelectric RT phase

The spontaneous polarization of the crystal was determined from the pyroelectric charge measurements. The crystal was poled while cooling down from the HT paraelectric phase to the 296 K RT phase in a constant electric field of 3.5 kV cm^{-1}. Then the pyroelectric charge was measured during the heating of the sample at a temperature rate of 2 K min^{-1}. The procedure of poling was repeated and then the pyroelectric charge was measured during the cooling. The spontaneous polarization was calculated by dividing the pyroelectric charge by the area of the sample. The temperature dependence of the spontaneous polarization (P_s) determined in this way is presented in figure 4 and shows that P_s continuously disappears at $T_1 = 336$ K, which is the Curie point. The abrupt change of the spontaneous polarization takes place at the discontinuous transition from the ferroelectric RT to the antiferroelectric LT phase. During the discontinuous phase transition the sample became milky and no further pyroeffect measurements were possible.

The magnitude of spontaneous polarization is determined as a sum of several components of the dipole moment present in the elementary cell. These components come from the pyridinium ring, the ReO_4 anion and from mutual displacement of the ions. On the basis of the structural data the dipole moments of the pyridinium ring and the tetrahedral ReO_4 ion were calculated using the Gaussian program. The dipole moment of the isolated pyridine ring was found as 1.97 D, which is in agreement with the results of [17]. As follows from NMR measurements [3], the pyridinium ring undergoes reorientations about its pseudo-hexagonal axis, which causes reduction of its dipole moment (figure 3). Knowing the occupancy probability p_i of the N atom from our structural data we calculated the reduced dipole

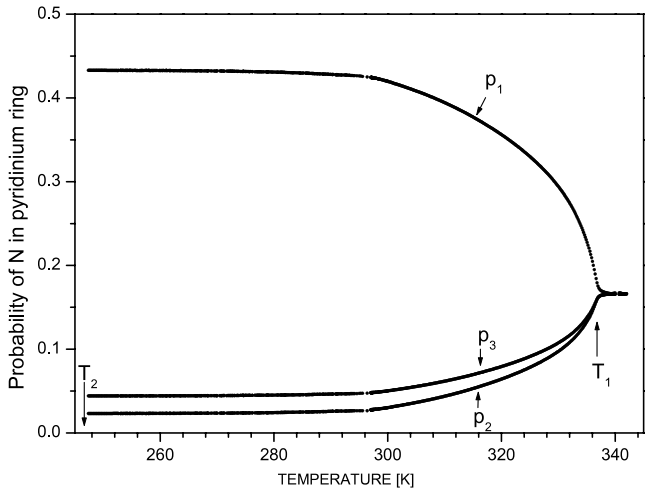

Figure 5. Calculated occupancy probability p_i of the nitrogen atom in pyridinium ring versus temperature in the RT and HT phases.

moment of the pyridinium cation and hence its contribution to the spontaneous polarization along the polar axis in the ferroelectric RT phase. The resultant spontaneous polarization coming from the pyridine rings in one elementary cell is $P_{sp} = 1.70\ \mu C\ cm^{-2}$.

As follows from our structural data, the tetrahedral ReO_4 anion has a small distortion that is the source of the dipole moment of 0.29 D, which generates a small component of this moment along the polar axis z; the relevant polarization component is $P_{sReO} = 0.06\ \mu C\ cm^{-2}$.

In the ferroelectric phase there is a small asymmetric shift of the ReO_4 anion centre and the pyridine ring centre, $\Delta z = 0.016$ Å along the polar axis and the spontaneous polarization component generated by this shift is $P_{sz} = 0.09\ \mu C\ cm^{-2}$ and its sign is the opposite to that of the component coming from the pyridine ring and the ReO_4 group.

The total spontaneous polarization at 300 K is the sum:

$$P_s = P_{sp} + P_{sReO} + P_{sz} \tag{5}$$

and its calculated value is $P_s = 1.67\ \mu C\ cm^{-2}$, which is in good agreement with the value obtained from the pyroelectric effect measurements, see figure 4.

As the spontaneous polarization component coming from the pyridinium ring dipole is $P_{sp} \gg P_{sReO}$ and its component coming from the shift is $P_{sp} \gg P_{sz}$, the ferroelectric crystal $PyReO_4$ should be classified as an order–disorder type with a very small contribution of the displacive type. That means that the spontaneous polarization in $PyReO_4$ depends mainly on the orientation of the pyridinium ring dipole and hence on the occupancy probability p_i on the nitrogen atom. Therefore temperature dependence of p_i will be similar to the temperature dependence of P_s. From our neutron diffraction studies we obtained the p_i values only at 350, 300 and 100 K. But having the P_s temperature dependence we can estimate the occupancy probability p_i for a wide range of temperature. The results are presented in figure 5. Similar calculations for pyridinium periodate were performed by Miyoshi [18].

At LT the pyridinium ring is fully ordered with $p_1 = 1$ (figure 3). The doubling of the a lattice cell parameter in the anti-parallel orientation of pyridinium dipole moments results in the disappearance of spontaneous polarization in the LT antiferroelectric phase.

4. Conclusions

(1) The neutron diffraction studies of $PyReO_4$ at 350, 300 and 100 K confirmed the x-ray results and allow for a detailed description of the symmetry and structure of the three polymorphs: $Cmcm \rightarrow Cmc2_1 \rightarrow Pbca$.
(2) In the paraelectric HT and ferroelectric RT phases the pyridinium cations exhibit an orientational disorder, while the ReO_4 anions are ordered. The antiferroelectric LT phase is fully ordered.
(3) The orientational disorder of the nitrogen atom of the pyridinium ring has been precisely described at 350, 300 and 100 K with the refined occupancy parameter p_i.
(4) On the basis of structural results the calculated entropy was compared with that obtained from DSC heat capacity measurements.
(5) The theoretically calculated spontaneous polarization value in the ferroelectric crystal phase was compared with that obtained from pyroeffect measurements.
(6) The dependence of the nitrogen atom p_i occupancy probabilities was calculated for a wide temperature range using crystal structure data and spontaneous polarization P_s measurements.
(7) In $PyReO_4$, $PyIO_4$ and $PyFCrO_3$ crystals there is a relation between the value of spontaneous polarization P_s and the size of the tetrahedral anion. The spontaneous polarization increases with the size of anion (table 3): $P_s \cong 1\ \mu C\ cm^{-2}$ in $PyFCrO_3$, [7], $1.6\ \mu C\ cm^{-2}$ in $PyReO_4$ and $3.5\ \mu C\ cm^{-2}$ in $PyIO_4$ [6].
(8) The $PyReO_4$ ferroelectric crystal can be classified as an order–disorder type with a very small contribution of the displacive type.

Acknowledgments

The experiments at LLB were supported by the European Commission through the Access Activities of the Integrated Infrastructure Initiative for Neutron Scattering and Muon Spectroscopy (NMI3), supported by the European Commission under the 6th Framework Programme through the Key Action: Strengthening the European Research Area, Research Infrastructures, contract no. RII3-CT-2003-505925.

References

[1] Czarnecki P, Nawrocik W, Pająk Z and Wąsicki J 1994 *Phys. Rev.* B **49** 1511
[2] Czarnecki P, Nawrocik W, Pająk Z and Wąsicki J 1994 *J. Phys.: Condens. Matter* **6** 4955
[3] Wąsicki J, Czarnecki P, Pająk Z, Nawrocik W and Szczepański W 1997 *J. Chem. Phys.* **107** 576
[4] Czarnecki P and Małuszyńska H 2000 *J. Phys.: Condens. Matter* **12** 4881

[5] Małuszyńska H, Czarnecki P, Lewicki S, Wąsicki J and Gdaniec M 2001 *J. Phys.: Condens. Matter* **13** 11053
[6] Małuszyńska H, Scherf C, Czarnecki P and Cousson A 2003 *J. Phys.: Condens. Matter* **15** 5663
[7] Pająk Z, Małuszyńska H, Szafrańska B and Czarnecki P 2002 *J. Chem. Phys.* **117** 5303
[8] Horiuchi S, Tokunaga Y, Giovannetti G, Picozzi S, Itoh H, Shimano R, Kumai R and Tokura Y 2010 *Nat. Lett.* **463** 789
[9] Horiuchi S, Fumiyuki I, Kumai R, Okimoto Y, Tachibana H, Nagaosa N and Tokura Y 2005 *Nat. Lett.* **4** 163
[10] Dawber M, Rabe K M and Scott J F 2005 *Rev. Mod. Phys.* **77** 1083
[11] Katrusiak A and Szafrański M 1999 *Phys. Rev. Lett.* **82** 576
[12] Szafranski M, Katrusiak A and McIntyre G J 2002 *Phys. Rev. Lett.* **89** 5507
[13] Scott J F 2005 *Ferroelectrics* **316** 13
[14] Sheldrick G 1997 *SHELXS-97 Program for Crystal Structure Determination* University of Goettingen
[15] Sheldrick G 1997 *SHELXL-97 Program for Crystal Structure Determination* University of Goettingen
[16] Hanaya M, Shibazaki H, Oguni M, Nemoto T and Ohashi Y J 2000 *Phys. Chem. Solids* **61** 651
[17] Beck B, Villanueva-Garibay J A, Müller K and Roduner E 2003 *Chem. Mater.* **15** 1739
[18] Miyoshi T, Kasano H and Mashiyama H 2007 *Ferroelectrics* **346** 130